Using in-situ viscosimetry and morphogranulometry to explore hydrolysis mechanisms of filter paper and pretreated sugarcane bagasse under semi-dilute suspensions

Tuan Le, Dominique Anne-Archard, Véronique Coma, Xavier Cameleyre, Eric Lombard, Kim Anh To, Tuan Anh Pham, Tien Cuong Nguyen, Luc Fillaudeau

Regular article

Using *in-situ* viscosimetry and morphogranulometry to explore hydrolysis mechanisms of filter paper and pretreated sugarcane bagasse under semi-dilute suspensions

Tuan Le[a,b,d], Dominique Anne-Archard[c,d], Véronique Coma[e], Xavier Cameleyre[a], Eric Lombard[a], Kim Anh To[b], Tuan Anh Pham[b], Tien Cuong Nguyen[a,b,d], Luc Fillaudeau[a,d,*]

[a] *Laboratoire d'Ingénierie des Systèmes Biologiques et des Procédés (LISBP), Université de Toulouse, INSA, INRA UMR792, CNRS UMR5504, 135 avenue de Rangueil, F-31077 Toulouse, France*
[b] *Center for Research and Development in Biotechnology (CRDB), Schools of Biotechnology and Food Technology (SBFT), Hanoi University of Science and Technology, 1 Dai Co Viet, Hai Ba Trung, Hanoi, Viet Nam*
[c] *Institut de Mécanique des Fluides de Toulouse (IMFT) – Université de Toulouse, CNRS-INPT-UPS, 2 Allée Camille Soula, F-31400 Toulouse, France*
[d] *Fédération de Recherche FERMAT (Fluides, Energie, Réacteurs, Matériaux et Transferts), Université de Toulouse, CNRS, INPT, INSA, UPS, Toulouse, France*
[e] *Laboratoire de Chimie des Polymères Organiques (LCPO), 16 Avenue Pey-Berland, F-33607 Bordeaux, France*

Keywords:
In-situ viscosity
Particle size distribution
Filter paper
Sugar cane bagasse
Enzyme
Hydrolysis

A B S T R A C T

The relationship between *in-situ* viscosimetry, *in-* and *ex-situ* morphogranulometry, and biochemistry has been investigated during enzymatic hydrolysis of pretreated sugarcane bagasse (SCB, 3% w/v) and filter paper (FP, 1.5% w/v) at various enzyme dosages (0.3–25 FPU/g cellulose). Semi-dilute conditions (1.5–2 times higher than critical concentrations) were considered in order to generate non-Newtonian rheological behaviors and to avoid neglecting particle–particle interactions in opposition to dilute conditions. Observed phenomena as well as hydrolysis mechanisms including solvation, separation, fragmentation, and solubilization appeared to depend strongly on initial substrate properties. For both FP and SCB, suspension viscosities were correlated with particle size distributions and volume fractions during hydrolysis, but they exhibited strongly different trends. With SCB, a viscosity overtaking was clearly observed at enzyme loading $\leq$10 FPU/g cellulose. This phenomenon is explained by the separation of agglomerates into individual fragments, leading to an increase in the total number of particles and a morphological shift of particles from sphere-like into fiber-like. With FP, the viscosity collapsed at the initial stage in relation to the volume reduction of coarse particles and the number increase of fine particles. Suspension viscosity was strongly dependent on the fraction of coarse population and nearly independent from the glucose conversion yield.

1. Introduction

Lignocellulosic feedstock is certainly the most abundant and the cheapest resource in the world [1]. It can consist of several agriculture and industry by-products such as sugarcane bagasse, rice straw, corn stove, and wood chips. Sugarcane bagasse is the lignocellulosic residue accumulated during the production of sugar. Chemically, bagasse contains about 50% cellulose, 30% pentosans, and 2.4% ash [2]. Because of the low ash content in chemical composition compared to other lignocellulosic biomasses such as rice straw (17.5% ash content) and wheat straw (11% ash content), sugarcane bagasse is a very promising feedstock for use in bioprocesses. According to Kim and Dale [3], the world global production of sugarcane is 328.10^9 kg, which corresponds to around

Abbreviations: CLD, chord length distribution; DLS, diffraction light scattering; d_{SE}, diameter of circle equivalent (μm); FBRM, focused beam reflectance measurement; FP, filter paper; FPU, filter paper unit; l_c, chord length (μm); LOD, limit of detection; LOQ, limit of quantification; MO, Metzner-Otto concept; *Nc*, number of chord counted (/); *Np*, power number (/); PP, paper pulp; PSD, particle size distribution; *Re*, Reynolds number (/); SCB, sugarcane bagasse.

* Corresponding author at: Laboratoire d'Ingénierie des Systèmes Biologiques et des Procédés (LISBP), CNRS UMR5504–INRA UMR792-INSA, 135 avenue de Rangueil, F-31077 Toulouse cedex 4, France.
E-mail addresses: tuan.le@insa-toulouse.fr (T. Le), dominique.anne-archard@imft.fr (D. Anne-Archard), veronique.coma@u-bordeaux.fr (V. Coma), xavier.cameleyre@insa-toulouse.fr (X. Cameleyre), eric.lombard@insa-toulouse.fr (E. Lombard), anh.tokim@hust.edu.vn (K.A. To), anh.phamtuan2@hust.edu.vn (T.A. Pham), cuong.nguyentien1@hust.edu.vn (T.C. Nguyen), luc.fillaudeau@insa-toulouse.fr (L. Fillaudeau).

http://dx.doi.org/10.1016/j.bej.2017.07.006

180.10^9 kg of dry sugarcane bagasse. This resource is an abundant source of raw material for biotransformation. Thus, the conversion of sugarcane bagasse to fuel ethanol has long been under consideration [4–6]. However, the processes proposed in these publications remain in laboratory scale and need to be optimized for industrial application.

In the bioconversion of lignocellulosic biomass, enzymatic hydrolysis is crucial because it transforms cellulose/hemicellulose fibers into fermentable substrate. In order to achieve a viable economy, the biotransformation of lignocellulose into monomer sugar has to be performed at high concentrations of raw material [7]. Working at high dry matter concentration, the challenges to solve are not only in the field of biochemistry but also extend to physical aspects. An increase in suspension viscosity leads to a rise in the energy needed for mixing. It also causes poor mixing capacity and limits mass transfer. Consequently, low enzyme distribution and localized hydrolysis can possibly occur. In order to overcome these difficulties, an investigation by physical approach is necessary to understand the mechanism of hydrolysis, as well as to identify key factors limiting conversion yield. To get in-depth knowledge, the biochemical and physical phenomena should be investigated simultaneously because of their strong coupling.

The physical research on lignocellulosic slurries started more than a decade ago [8–12]. It includes several analyses, such as suspension viscosity, yield stress, particle morphology characterization, crystallinity, porosity, surface properties, and polymerization degree. Properties of mass and heat transfer, rheological behavior of suspensions, particle morphology and fiber degradation mechanisms appeared as determinant factors of the effectiveness of the process. Lignocellulosic suspensions exhibit non-Newtonian behavior (shear-thinning, viscoplasticity). Suspension viscosity and yield stress strongly depend on substrate concentration and particle size and shape distributions. It is reported that reducing particle size may improve enzymatic hydrolysis efficiency and reduces the viscosity of biomass slurries [13,14]. The literature reports on the physical properties (yield stress, viscosity, particle size distribution (PSD)) of fiber suspensions at the initial stage [15–17] and during enzymatic hydrolysis [16,18–20]. A decreasing trend in overall conversion yield with increasing solids loading has been reported for several lignocellulosic substrates [21–23]. At high solid concentration, the physical limitations become a sticking point and need to be scrutinized.

A decreasing trend in overall conversion yield with increasing solids loading has been reported for several lignocellulosic substrates [21–23]. At high solid concentration, the physical limitations become a sticking point and need to be scrutinized. The rheological understanding of lignocellulosic suspensions is fundamental to the optimization of process efficiency [10,24]. Through the bibliography analysis, there is only 3 publications that investigates in parallel the biochemical, morphological and *in-situ* [16] and *ex-situ* [25,26] rheological approaches. Aiming to complete this knowledge, and for further research on high dry matter conditions, our strategy was to investigate enzymatic hydrolysis at semi-dilute conditions to understand the fragmentation and solubilization mechanisms. The relationship between *in-situ* viscosimetry and biochemistry was specifically scrutinized during hydrolysis of two substrates – pretreated sugarcane bagasse (SCB 3% w/v) and milled filter paper (FP 1.5% w/v) – by a commercial cocktail (Ctec2–Novozyme). These concentrations were 1.5–2 times higher than critical concentrations (previously identified [16]), which led to non-Newtonian suspension behaviors. Consequently limited particle–particle interactions occurred contrary to dilute conditions, but without the highest complexity of high dry matter contents. This controlled complexity enabled further exploration of the physical limitations during hydrolysis of cellulosic substrates. Various enzyme-to-substrate (E/S) ratios (0.3–25 FPU/g cellulose) were studied with a multi-instrumented experimental set-up. Semi-dilute conditions and low activities (0.3–3 FPU/g cellulose) highlighted specific phenomena such as viscosity overtaking and magnitude of particle fragmentation *versus* solubilization. These operating conditions provided slow hydrolysis kinetics that facilitated observation and characterization of the phenomena at macroscopic (viscosimetry), microscopic (granulometry) and biochemical (sugar concentration) levels. Moreover, these conditions allow negating end-product inhibition, minimizing the transfer limitations, homogenizing enzyme and suspension distributions.

First, biochemical and physicochemical properties of initial suspensions are compared. Second, hydrolysis rates and viscosity are discussed as a function of the E/S ratio. Then, the final step focuses on PSD and chord length distribution (CLD) analysis, with exploration of the particle size evolution under enzymatic reaction in relation to glucose conversion yield and suspension viscosity.

2. Materials and methods

2.1. Substrates and enzymes

Pretreated sugarcane bagasse (SCB) obtained from the Center of Research and Development in Biotechnology, SBFT-HUST, Hanoi, Vietnam (CRDB), was used as real lignocellulose substrate. Raw bagasse was collected from the Lam Son Sugar factory (Thanh Hoa, Vietnam), then pretreated using the organosolv process (thermochemical pretreatment using formic acid). It was deformylated by diluted NaOH and washed until neutral pH. Pretreated SCB was extruded to homogenize the particle size (EuroLab 16 Extruder, 400 mm failure, extrusion line: 25 L/D 18/25 conveying, 7/25 shear stress). Extruded SCB was stored at 4 °C until use (dry matter content ~25%). Its chemical composition consisted of 4.5% hemicellulose, 79.9% cellulose, 1.4% lignin. The analysis was performed using FibertecTM following the Van-Soest method [27].

Dried and milled (Bosch MKM6003 mill) filter paper (Whatman International Ltd., Maidstone, England, Cat No. 1001 090) was selected as reference for cellulosic substrate. The composition of filter paper (FP) was 99.68% cellulose. It did not contain hemicellulose.

Surface tension analysis showed interfacial interaction free energy (ΔG_{SES}) of 34.2 mJ/m^2 and 6.44 mJ/m^2, and hydration free energy (ΔG_{SE}) of −146.3 mJ/m^2 and −130.1 mJ/m^2 respectively for FP and SCB. Analysis was carried out using a Drop Shape Analyzer DSA-100 (KRUSS) following tangent and Young-Laplace methods. These results proved the similar hydrophilic properties of both substrates.

With increasing concentration, both FP and SCB suspensions behaved in an increasingly non-Newtonian way. A critical concentration specific to each substrate can be observed [28]; this concentration is defined as the passage from dilute behavior (substrate concentration has minor effect on suspension viscosity) to semi-dilute and concentrated behavior (substrate concentration greatly influences suspension viscosity and non-Newtonian behavior). Rheological behavior of suspensions was investigated at 40° C, with substrate concentration varying up to 15 g/L for FP and 53 g/L for SCB. The mixing rate was in the range of 20–250 min^{-1}. The critical concentration was identified as 7 g/L for FP and 23.9 g/L for SCB.

The enzymatic cocktail used was Cellic Ctec2 from Novozymes (Serial 0139 batch VCN10002), which is a commercial lignocellulase cocktail. Protein concentration was 64.8 ± 4.7 mg/mL following Bradford assay and Bovine Serum Albumin (BSA) as standard. Enzy-

matic activity and thermo-stability were characterized in specific conditions (T = 40° C, pH = 4.8) following the IUPAC method [29].

One unit of filter paper (FPU), endoglucanase (CMCU) and exoglucanase (AVCU) activities [30] equal to the amount of enzyme to release 1 μmol/min of glucose as reducing sugar from respectively 50 mg filter paper, 2% CMC (carboxyl methyl cellulose, degree of substitution 7 M) and 2% Avicel suspension (micro-crystalline cellulose 90 μm). One unit of cellobiase activity (CBU) is equivalent to the amount of enzyme to release 2 μmol/min of glucose from 15 mM cellobiose.

Activities per mL of cocktail are equal to 103 FPU, 104 AVCU, 831 CMCU and 3796 CBU. Enzyme was stored at 4 °C until used. Enzyme dosage in hydrolysis experiments was based on FPU per gram of cellulose on dry weight basis.

2.2. Experimental setup

The experimental setup includes a double jacket glass bioreactor (d = 130 mm, H = 244 mm, V = 2.0 L) equipped with a home-designed impeller system associated with several *in-situ* sensors (temperature, pH, rotation speed, torque, FBRM). The impeller is an assemblage of two classical ones, mounted on the same shaft. The first one is a three inclined blades (diameter: 73.5 mm, angle: 45°, h = 38 mm) located at 75 mm height from the bottom to ensure mixing in the central region of reactor as well as suspension homogeneity. The second is a close bottom mixer including 2 large blades (diameter: 120 mm, h = 22 mm) to avoid substrate decantation. A Haake VT550 viscometer (Thermo Fisher Scientific ref: 002-7026) was used to ensure mixing at specific rotation speed as well as *in-situ* torque measurements. The temperature was controlled by water circulation (combined cryostat Haake DC30-K20, Thermo Fisher Scientific) through the water jacket of the bioreactor. The viscometer and the cryostat were controlled by original software from Haake (RheoWin Job Manager) that also ensured real-time data recording (temperature, torque, mixing rate). The pH of the suspension was controlled and auto-adjusted by a Biostat-B (Sartorius Stedim Biotech) *via* home-designed software created in the LabVIEW environment. Finally, a focused beam reflectance sensor (FBRM-G400-Mettler Toledo) was located inside the reactor in order to measure the distribution of particle chords. A global description of the whole system is illustrated in Fig. 1.

2.3. Chemical and physical analysis

2.3.1. Mono- and disaccharide concentrations

Mono- and disaccharides were analyzed using high-performance liquid chromatography (HPLC, Agilent Technologies, 1200 series). Measurements were performed on an Aminex HPX-87P column #1250098 with micro-guard Carbo-P refill cartridges #1250119 (both from Bio-Rad). Separation was carried at flow rate 0.5 mL/min, column temperature 60 °C using HPLC-grade water (LiChrosolv, Merck) as mobile phase and refractive index detector. All samples were centrifuged at 10,000 min^{-1} for 10 min, then filtered through 0.22 μm filters before injection into the column. Calibration curves were established with standard solutions of cellobiose, glucose, xylose, arabinose, galactose, and mannose (concentration ranging between 0 to 1 g/L). The lower and upper LOD are equal to 0.01 and 1 g/L respectively and the LOQ is equal to 0.036 g/L.

2.3.2. Dry matter content and volume fraction

The water content of substrates and hydrolyzed suspensions was determined by drying at high temperature and ambient pressure. A known mass of sample (m_1 equivalent to 1–3 mL) was filtered through filter paper (Whatman paper N°1, known mass, m_0), then placed in the oven at 105 °C, for 12 h and weighed up to constant mass (m_2). Water content (W) and dry matter (DM) were then calculated from these measurements with an accuracy of ±2%. The volume fraction (Φ_V) is defined as the volume of particles (V_p) divided by the volume of whole suspension ($V_{sus} = V_p + V_{water}$) prior to mixing. In the present work, this volume fraction is calculated from mass balance by considering the initial concentration, the hydrolysis yield and particle density. ρ_{DM} and x_{DM} are respectively particle density (g/L) and water-insoluble fraction (g).

$$\Phi_v = \frac{V_p}{V_{sus}} = \frac{x_{DM}/\rho_{DM}}{V_{sus}} \tag{1}$$

2.3.3. In-situ *viscosimetry*

In-situ viscosimetry was conducted throughout hydrolysis, based on the real-time monitoring of torque and mixing rate and using the Metzner-Otto concept when fluids are non Newtonian ones [31].

In laminar flows and for Newtonian fluids, the product of the Reynolds number (*Re*) by the Power number (*Np*) is constant and usually written as:

$$Np = Kp \cdot \frac{1}{Re} \tag{2}$$

The power consumption curve, $Np = f(Re)$ was characterized using Newtonian reference fluids—distilled water, glycerol, and Marcol 52 oil (Exxon Mobil). Eq. (2) for laminar regime can be extended to turbulent ones (until a critical *Re* value) and described by a unique equation: Eq. (3).

$$Np = \left[\left(\frac{Kp}{Re}\right)^{\alpha} + Np_0^{\alpha}\right]^{1/\alpha} \tag{3}$$

Kp and α are two constants that only depend on the mixing system geometry. Np_0 is the power number for turbulent flows. Experimental results on our system gave $Np_0 = 0.017$, $\alpha = 0.75$, $Kp = 115.2$ and shown that a laminar regime prevailed up to $Re = 41$.

When fluids are non-Newtonian, Eq. (3) is still valid as long as a generalized Reynolds number is used. This last one is calculated using the Metzner-Otto (MO) concept which allows the determination of an equivalent viscosity from the rotation frequency. The MO concept introduces a constant *Ks* which only depends on geometrical characteristics of the mixing system. *Ks* was determined experimentally using 0.04%–0.1% shear-thinning xanthan solutions prepared in a saturated solution of glucose and saccharose as reference fluids. The *Ks* value of our system is equal to 32. The concept can be extended up to transition flow [32]. In this study, the application of a power consumption curve to calculate suspension viscosity and establish an *in-situ* rheogram was extended to transitional flow, which is equivalent to $Re < 1000$. In turbulent flow, the power consumption curve is limited to viscosity determination, but limited up to $Re = 30000$ (beyond this value, *Np* is almost constant). Detailed methodology was previously described [16].

2.3.4. Ex-situ *diffraction light scattering (DLS)*

The volume-weighted particle size distribution (PSD) was determined by diffraction light scattering (DLS, Mastersizer 2000, Malvern Inst., range from 0.02 to 2000 μm, red λ = 632.8 nm and blue λ = 470.0 nm light) using Mie scattering theory. A known volume of suspension (0.5–3 mL) was added to a water circulation loop (20 °C ± 2) in order to obtain laser obscuration between 5% and 40%. The whole suspension was mixed by a Heidolph magnetic stirrer at 200 min^{-1} while the circulation loop was maintained by a Masterflex L/S model 7553-79 at pump speed 240 min^{-1}. For each sample, measurements were performed in triplicate for 3 dilution rates and the average result was taken.

Laser diffraction analysis converts the detected scattered light into a PSD. This method involves measurement based on volume

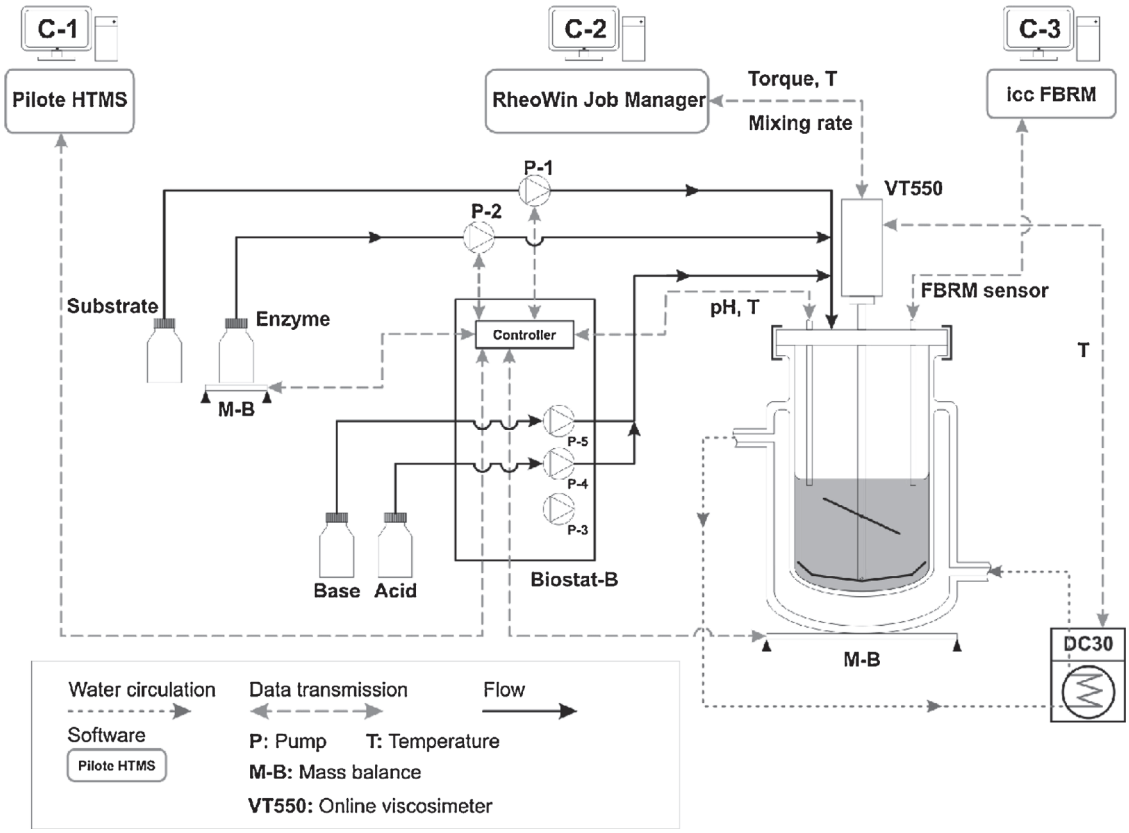

Fig. 1. Process and instrumentation diagram of experimental setup.

and identifies a diameter of equivalent sphere, d_{SE}. This interpretation of DLS measurements is based on strong assumptions, namely spherical particle shape and a known refractive index. For our substrates (fibrous shape and multimodal distribution), it suffers from a significant deviation compared to the ideal case. Nevertheless, the equivalent sphere diameter was used and will be discussed under these restrictions. Volume-weighted particle size distribution (E_v) was calculated by the Mastersizer software and then weighted by volume fraction (Φ_v) in order to integrate the impact of solubilization on suspended population and to allow comparison between distributions at different hydrolysis times.

2.3.5. In-situ *focus beam reflectance measurement (FBRM)*

Focus beam reflectance measurements enable *in-situ* quantification and characterization of chord length distribution (CLD). *In-situ* CLD of particles was analyzed using an FBRM® G400 probe (Mettler Toledo, range: 0.1–1000 μm, laser light source λ = 795 nm, laser source rotation: 2 m/s). This probe was placed in the reactor and allowed for real-time tracking of chord length and particle count during enzymatic hydrolysis. However, operating conditions (mixing rate, suspension viscosity) that affect flow pattern may also influence the count number. Thus for N_c, discussion and comparison will be restricted to almost constant viscosity phases. Thousands of individual chord lengths are typically measured each second to produce the number-weighted CLD, which is the fundamental measurement provided by FBRM®. The conversion from number-weighted CLD into volume-weighted PSD is possible under severe assumptions [33], but they are inappropriate for FP and SCB substrates because they contain particles of various shapes and dispersed sizes. Consequently, the number-weighted CLD, $E_n(l_c)$, and the average number of chords counted per second, N_c, will be used as indicators of population evolution. In order to facilitate comparison between experiments, normalized parameters were defined as the ratio between instantaneous value and initial value at t = 0 h

Normalized mean chord length:

$$l_c^*(t) = \frac{l_c(t)}{l_c(t=0h)} \tag{4}$$

Normalized total chord count:

$$N_c^*(t) = \frac{N_c(t)}{N_c(t=0h)} \tag{5}$$

Furthermore, as native measurements are number-based, the underrepresented classes in widespread population may become non-significant. This will be the case for the largest particles with FP and SCB substrates.

2.4. Operating conditions and protocols

Experiments were performed at 1.5% w/v for FP, and at 3% w/v for SCB. These concentrations are 1.5–2 times higher than critical concentration, in order to work with non-Newtonian behaviors. These conditions generate particle–particle interactions, which give rise to the complexity emanating from high dry matter contents.

The enzymatic reactions were carried out over 24 h at 100 min^{-1}, 40 °C, pH 4.8 ± 0.2 with a total volume 1.3 L. Enzyme-to-substrate ratios (E/S) were adjusted from 0.3 to 25 FPU/g cellulose. An antibiotic (1.3 mL of chloramphenicol 50 g L^{-1}) was added to prevent microbial contamination. Experiments were divided into two steps: i) homogenization of the suspension, and ii) enzymatic hydrolysis. In the first step, the material was mixed with water at 100 min^{-1} for a given duration (2–3 h) in order to achieve a homogeneous suspension and constant torque. In the second step, enzymes were added (at time t = 0) and *in-situ* measurements

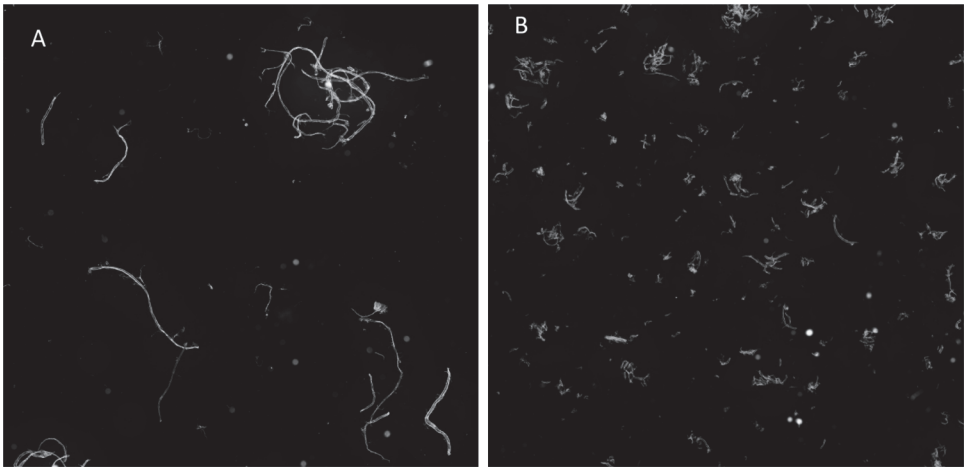

Fig. 2. Microscopic observation of FP suspension, 1.5% w/v (A), and SCB suspension, 3% w/v (B), both captures represent an area of 0.5 cm × 0.5 cm, 10× magnification, dark field mode (Morphologi G3S, Malvern Inst.).

(torque, pH, T, CLD) made. In the results presentation, knowing the non-Newtonian behavior of suspensions, one specific value of viscosity was chosen to track the time evolution of hydrolysis, namely the viscosity at 100 min^{-1}. Moreover, the non-Newtonian behavior was investigated every 30 min by repeating the cycle: (i) mixing at 100 min^{-1} for 28 min, (ii) shifting at 125 min^{-1} for 1 min, and (iii) linear slowdown to 100 min^{-1} in 1 min. Data acquisition period was adjusted to 1 min at 100 min^{-1} and decreased to 10 s in other conditions. Mean data were recorded in each period. During the step at 125 min^{-1} (1 min), mean values were calculated for stabilized torque. Samples (20 mL) were taken at 0 h, 1 h, 2 h, 3 h, 6 h, 12 h, 18 h and 24 h for biochemical and granulometric analysis.

3. Results and discussion

3.1. Comparison of initial suspensions

To evaluate the reproducibility of experimental conditions and the differences between FP and SCB, morphogranulometry and viscosity were specifically scrutinized. The morphogranulometric properties were investigated *via* different analyses: (i) microscopic observation provided qualitative information about particle shape and size, (ii) DLS measurements were well adapted to coarse particle fraction (volume distribution), and (iii) focused beam reflectance measurements highlighted the fine particle population (number distribution).

Microscopic observations of FP and SCB suspensions (Fig. 2A, B) show complex mixtures of coarse and fine particles with different morphologies and ratios. For FP suspensions, Fig. 2-A indicates a majority of long cellulosic fibers that are crossed or separated, with a large fiber length-to-diameter ratio. For SCB suspensions, the particle size appears generally smaller than for FP. The proportion of fine particles seems to be higher for SCB suspensions.

Volume-weighted distributions of equivalent sphere diameter are reported in Fig. 3-A for FP and SCB suspensions. FP suspensions show a multimodal population of coarse particles (46% with $d_{SE} > 200\ \mu m$) and fine particles (54% with $d_{SE} < 200\ \mu m$), whereas fine particles with $d_{SE} < 200\ \mu m$ represent 94% of the population for SCB. The volume-weighted diameters, d(v,0.1), d(v,0.5), d(v,0.9), corresponding to 10%, 50%, and 90% of the population, are 9.8 ± 0.3, 43.5 ± 1.8, $161.3 \pm 3\ \mu m$ for SCB and 20.9 ± 0.8, 169.4 ± 18.8, $1153.7 \pm 71.9\ \mu m$ for FP. Volume-weighted mean diameter D(4,3) of FP ($412.4 \pm 34.4\ \mu m$) is approximately 6 folds higher than for SCB ($71.4 \pm 1.3\ \mu m$).

Number-weighted CLD are illustrated in Fig. 3-B. The difference of size range between FP and SCB is noticeable with an expected shift to smaller dimensions. Both populations range between 1 to 200 μm. Mean chord lengths of $25.1 \pm 0.47\ \mu m$ and $16.4 \pm 0.43\ \mu m$ were reported for FP and SCB respectively. A slight shoulder is observed for FP.

In volume-weighted distributions, few coarse fibers may account for a large volume fraction, whereas they will be negligible when considering a number-weighted distribution. This is exacerbated with multimodal distributions with high size differences between fine and coarse subpopulations.

Considering the initial suspension viscosity measured at 100 min^{-1}, large differences were observed between FP and SCB that cannot be explained by surface tension and hydrophobic/hydrophilic properties. Particle size dispersion needs to be carefully considered, as it strongly affects suspension rheology. Strongly different behaviors may be exhibited between mixtures of hard sphere populations (ideal case with monodisperse particles) [28,34] and complex shape populations (real case with broad size distribution — spreading — and complex mechanical properties) [11,13,16]. For mixtures of hard spheres (D = 33–236 μm for glass beads and D = 84–141 nm for latex beads) with narrow distribution at a given volume fraction, monomodal suspensions have a higher viscosity than bimodal suspensions. This relationship was demonstrated on both Brownian and non-Brownian hard spheres for various diameter ratios from 2.7 to 22.1. The minimal viscosity is attributed to the presence of small particles between the larger ones in bimodal suspensions. In that way, at a given concentration, if the fiber length grows, the interaction probability between particles increases, especially due to entanglement, and this generates an increase in viscosity [33]. Suspension viscosity is controlled by particle concentration, but also by parameters such as morphological aspects (aspect ratio, shape, size, *etc.*), agglomerates and particle entanglement, surface properties, swelling propensity, and deformation capability [33,35–38] These numerous parameters lead to an ambiguous and hardly quantifiable definition of particle volume fraction. In this context, results reported by Dasari and Berson [13] indicated correlation between particle size and suspension viscosity with sawdust without considering this complexity. The same observations were stated by Viamajala et al. [11] with pretreated corn stover slurries, and Nguyen et al. [16] for concentrated cellulose fiber suspensions. Viscosities and PSD of FP and SCB suspensions were in agreement with this last assumption considering the relation between suspension viscosity and PSD.

Investigation of suspension viscosity as a function of mixing rate confirms non-Newtonian shear-thinning behavior. The mean viscosities of FP suspension decreased from 0.249 Pa s at 100 min^{-1} to

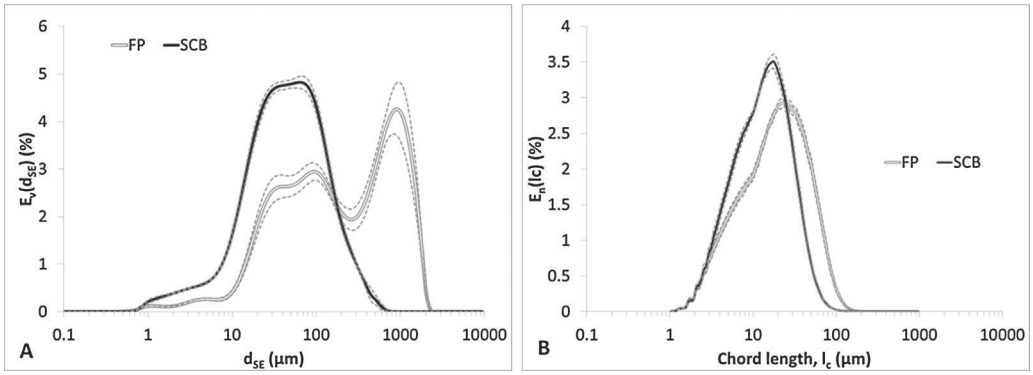

Fig. 3. Volume distributions of sphere equivalent diameter by DLS measurements (A) and number distribution of chord length by FBRM (B) for FP and SCB (dotted lines: average deviation issued from at least 6 experiments).

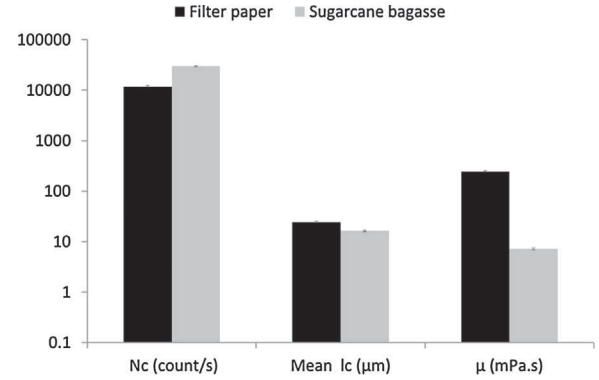

Fig. 4. Initial count number (N_c), mean chord length (l_c), and suspension viscosity (μ) for FP at 1.5% w/v and SCB at 3% w/v. Error bar represents the average of the absolute deviations from their mean.

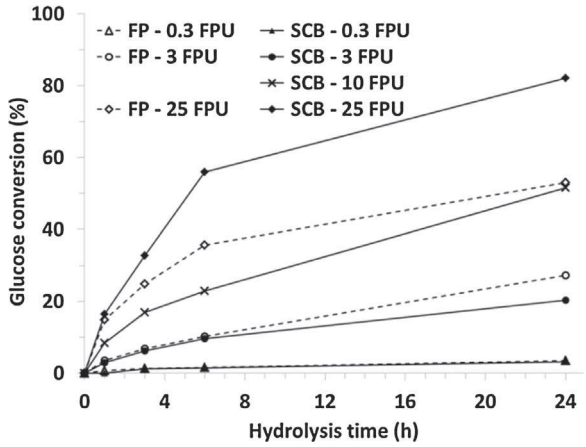

Fig. 5. Glucose conversion yield of all experiments.

0.183 Pa s at 125 min^{-1}. This behavior is largely reported in literature [33,39].

Fig. 4 reports initial values of size and viscosity for the different experiences with FP and SCB suspensions. It illustrates the reproducibility of these measurements. For FP, the deviations are equal to 5.4% and 3.5% for count numbers and mean chord length respectively. These same numbers for SCB are 1.9% and 2.6%, indicating good reproducibility between experiments. The same accuracy is observed for the viscosity of initial suspensions, with deviation of 2.8% and 6.2% for FP and SCB respectively.

3.2. *Hydrolysis rates*

Experiments were conducted for enzyme-to-substrate ratios ranging from 0.3 to 25 FPU/g cellulose. The bioconversion yields from cellulose into glucose after 24 h hydrolysis varied to a large extent as illustrated in Fig. 5. Our research strategy was not to reach the highest yields but to observe physical phenomena under limited and controlled hydrolysis conditions. Thus, the characterization of rheological and morphogranulometric properties during enzymatic reaction at different levels of substrate solubilization was considered. At 0.3 FPU/g cellulose, the bioconversion rates were negligible and equal to 3.5% and 3.1% for FP and SCB respectively. As the conversion rate stayed very low, the variation of substrate concentration during hydrolysis at 0.3 FPU/g cellulose can be neglected. Up to 3 FPU/g cellulose, the hydrolysis yields were almost similar between the two substrates. However, at the highest dosage (25 FPU/g cellulose), it is reported that FP was less accessible to enzymes than SCB, and the glucose yields after 24 h reached respectively 50.1% and 82.1% for their suspensions. These results are in good agreement with the morphogranulometric properties of the initial suspension (§3.1), as SCB suspensions contain a majority of short fragments enhancing specific surface.

3.3. In-situ *viscosimetry*

The time-viscosity curves of FP and SCB suspensions during hydrolysis for various Ctec2 ratios are reported in Fig. 6A and B. These curves demonstrate the ability to finely quantify *in-situ* viscosity during bio-catalysis, even for low values (SCB). The reference curves (no activity) demonstrate the absence of significant change in viscosity over 24 h. With enzyme activities, the curves fulfill a dose-effect response, but in a non-linear mode. However, the evolution and the curve shapes strongly differ between FP and SCB. These trends and differences are exacerbated with the lowest E/S ratios.

With FP suspensions, a monotone decrease of viscosity is observed, and this decrease is all the more rapid because enzyme loading is high. At 25 FPU/g cellulose, the FP suspension was liquefied in a short time: after 1 h hydrolysis, viscosity was only 5.8% of its initial value. At 3 FPU/g cellulose, it took 3 h to observe a 90% reduction in viscosity. In both cases, when hydrolysis was carried out, the suspension viscosity quickly reached the supernatant (water) viscosity. Turbulent flow regime was then rapidly established, and the estimation of *in-situ* viscosity was poorly reliable. The same limitation during *ex-situ* rheometry was encountered by Rosgaard et al. [40] with steam-pretreated barley straw, due to a shift in turbulent flow at high shear rates. At 0.3 FPU/g cellulose, the viscosity decline was slower and longer, even after 12 h of hydrolysis. A final viscosity of 0.09 Pa s was observed, equivalent to a decrease of 64% compared to the initial value.

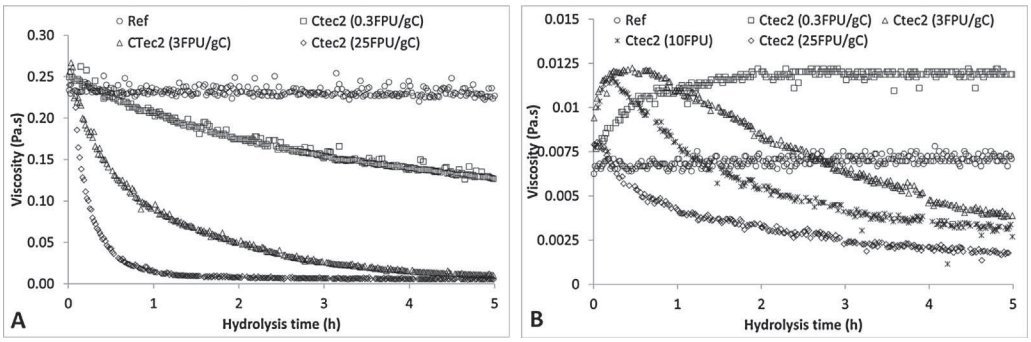

Fig. 6. *In-situ* viscosity during the first 5 h of hydrolysis of FP suspensions 1.5% w/v (A) and SCB suspensions 3%w/v (B) using Ctec2 cocktail at different dosages (0–25 FPU/g cellulose).

During enzymatic hydrolysis at 3 FPU/g cellulose, the FP suspension preserved its shear-thinning properties. The ratio of viscosity between 100 min^{-1} and 125 min^{-1} fluctuated around 1.35–1.41 from the beginning up to 10 h. The shear-thinning behavior of the reaction medium was then roughly constant during this period and did not seem to be drastically modified. Beyond this point, viscosity calculation was forbidden due to the appearance of the turbulent regime. For SCB, similar analysis was not performed because of the low magnitude of viscosity at 100 and 125 min^{-1}, which did not ensure accurate calculation.

It is noticeable that the liquefaction (viscosity reduction) is not directly related to the hydrolysis (glucose) yield. At 25 FPU/g cellulose, the glucose yield was only 14.8% after 1 h hydrolysis, while viscosity was reduced by 94.2%. From 1 h until 24 h, no evolution in suspension viscosity was observed, whereas glucose yields increased gradually up to 53.0%. At 3 FPU/g cellulose, a similar assessment was established with 6.8% glucose yield after 3 h, which corresponded to a 90% reduction in viscosity. Beyond 3 h, the glucose yield increased up to 24.8%. Liquefaction kinetics were higher than solubilization ones, whatever the operating conditions. The hydrolysis of cellulosic fiber consists of three actions associated with enzyme activities present in the cocktail. The random breakage of high-DP molecules into smaller ones by endoglucanase facilitates exoglucanase activity (attacking fibers from their ends and liberating cellobiose). Then β-glucosidase finally works on the conversion of cellobiose into glucose and has a minor effect on suspension viscosity but greatly increases hydrolysis yield. Obtained results prove that for semi-dilute conditions, liquefaction is a preliminary step for glucose production. At higher solid loading, when physical limitation becomes predominant, the role of liquefaction might be exacerbated.

With the SCB suspension (Fig. 6A), the time evolution of viscosity strongly differs and exhibits an initial overtaking before decrease. With the reference experiment (no enzyme added), a slight and linear increase in suspension viscosity by less than 15% after 24 h was observed. At enzyme loading ranged between 0.3 and 10 FPU/g cellulose, a significant increase in suspension viscosity at almost the same magnitude was witnessed during the first stage of hydrolysis. This was then followed by a stable or decreasing trend depending on the E/S ratio. Compared to the reference experiment (no activity), the viscosity overtaking then results from enzyme activities on SCB. At 0.3, 3, and 10 FPU/g cellulose, the glucose conversion yield at excess points was insignificant and equal to 1.2%, 2.9%, and 1.9%, respectively. Therefore, the substrate concentration cannot explain the evolution of suspension viscosity. A swelling effect of paper pulp, which is gradually hydrated, was suspected to explain this viscosity overtaking, but no conclusion can be stated on the basis of the results that have been presented. Basically, the enzymatic hydrolysis of lignocellulosic materials causes viscosity decrease *via* two mechanisms, including the fragmentation of coarse particles and the solubilization of fine particles. The viscosity excess under enzymatic action appears to be incomprehensible following a biochemical approach. Its interpretation requires further investigation of physical parameters, such as particle size and/or shape, in order to propose coherent mechanisms.

3.4. Granulometric analysis

As expected, a shift to smaller dimensions was observed during hydrolysis. Considering the influence of different physical factors on suspension rheological behavior, the volume-weighted PSD as well as the particle volume fraction (Φ_v) were specifically scrutinized and discussed. Meantime, the chord number N_c and the number-weighted CLD of particles, $E_n(l_c)$, will provide specific information about the evolution and contribution of the finest population. DLS (§2.3.4) and FBRM (§2.3.5) have specificities and limitations in relation to the volume- and number-weighted distributions that constitute the raw measurements. Their complementarity will be used to investigate changes in coarse and fine populations.

3.4.1. Particle size distribution during enzymatic hydrolysis

In order to allow comparison of particle size, PSD was weighted by the particle volumetric fraction (Φ_v), taking into account the reduction of suspended matter by solubilization during the process. For FP suspensions, Fig. 7 reports two E/S ratios at 3 and 25 FPU/g cellulose in order to examine slow and rapid viscosity evolutions. For SCB suspensions, Fig. 8 reports 0.3 and 3 FPU/g cellulose, considering a focus on viscosity overtaking.

For FP, as previously reported in Fig. 3A, the initial PSD exhibits a large, bimodal spreading distribution of 54% fine ($d_{SE} < 200\ \mu m$) and 46% coarse ($d_{SE} > 200\ \mu m$) populations. Results from DLS analysis (Fig. 7A and B) highlight the fragmentation mechanism on the coarse population at all tested dosages. This suggests a transition into fine population at a magnitude depending on the amount of enzyme loaded. However, the increase in volume-weighted distribution of the fine population was not as strong as expected. It may be due to the fact that DLS measurements based on volume-weighted distribution are probably less sensitive to fine particles. On the other hand, concomitantly with the increase of the fine population by fragmentation of the coarse population, the solubilization mechanism possibly affects and balances the fine population. The evolution of the fine population will be scrutinized deeply following number-weighted distributions using FBRM (see §3.4.2).

At 25 FPU/g cellulose (Fig. 7B) and after 1 h, $E_v(d_{SE}) \times \Phi_v$ indicates a transition from coarse to fine population. The total volume-weighted of coarse population, $\Phi_{v-coarse}$ decreases by 46.3% from t = 0 h to t = 1 h. Simultaneously, the volume fraction of the fine population Φ_{v-fine} increases by 9.4%. These size and vol-

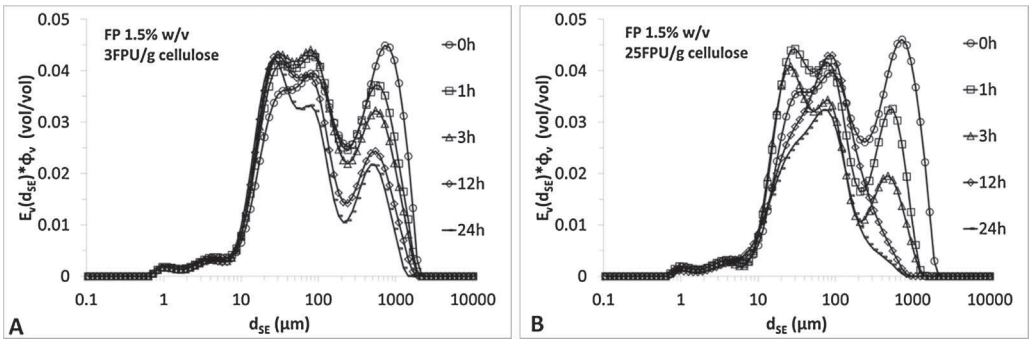

Fig. 7. Particle size distribution weighted by particle volume fraction during hydrolysis of FP suspensions for two enzyme loadings (A: 3 FPU/g cellulose, B: 25 FPU/g cellulose).

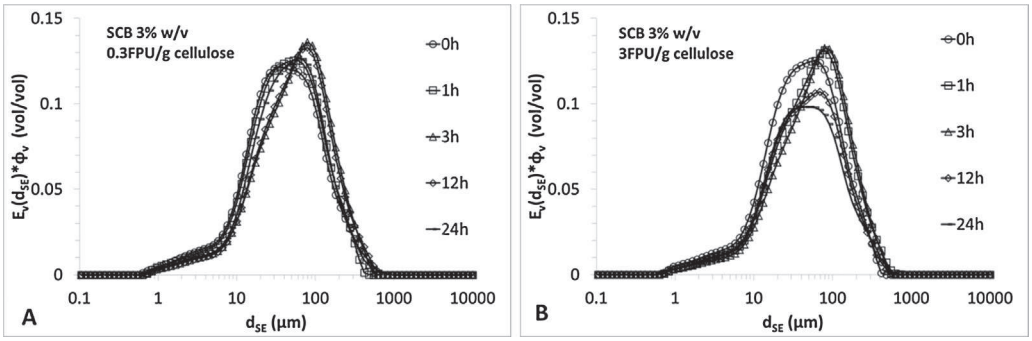

Fig. 8. Particle size distribution weighted by particle volume fraction during hydrolysis of SCB suspensions for two enzyme loadings (A: 0.3 FPU/g cellulose, B: 3 FPU/g cellulose).

ume evolutions correspond to a viscosity collapse of 94.2% (Fig. 6). Beyond 1 h, in parallel with the decrease in coarse population, a significant reduction of fine particle fraction by 45.3% was observed when comparing 1 h and 24 h. However, nearly no change in suspension viscosity is reported during this period. The reduction of total particle volume fraction is correlated to substrate solubilization, as indicated by the increase of glucose yield from 14.8% (t = 1 h) to 53.0% (t = 24 h).

At 3 FPU/g cellulose, similar trends were observed with slower kinetics. Between 0 h and 3 h, 38.2% viscosity reduction was observed, which corresponds to a 26.5% decrease in coarse population (from 0.0053 to 0.0043 for $\Phi_{v-coarse}$), whereas a 12.5% increase in fine population (from 0.0071 to 0.0079 for Φ_{v-fine}). At 3 h, the conversion yield of cellulose into glucose remains inferior to 6%, meaning that no significant change in total particle fraction (from 0.0124 to 0.0116 for Φ_V) was observed. Beyond 3 h, the reduction of coarse and fine populations was demonstrated in association with viscosity reduction up to 75.9% at 24 h. Meanwhile, the glucose conversion yield increased from 5% (t = 3 h) to 28.3% (t = 24 h). At 0.3 FPU/g cellulose (data not shown), similar phenomena were observed, with the coarse population decreasing in volume fraction, whereas negligible changes were reported for the fine population.

Szijarto et al. [41] reported the dominant role of purified endoglucanase in the liquefaction of pretreated wheat straw slurries. This activity randomly breaks the high DP chains into shorter fragments and causes a quick decrease in suspension viscosity. In our conditions, and assuming that the initial hydrolysis step is controlled by endoglucanase activity on the coarse population, the evolution of viscosity and PSD weighted by particle volume fraction (Φ_V) appears consistent with this assumption in increasing the number of ending chains. However, granulometric and biochemical mechanisms result from a complex balance between coarse and fine populations taking into account microscopic properties up to biochemical structure. Afterwards, the action of exoglucanase and β-glucosidase become more and more significant, leading to an increase in glucose conversion yield and a decrease in the fraction of fine particles.

By hydrolyzing substrate at low E/S loadings (0.3 and 3 FPU/g cellulose), the fraction of coarse particles ($d_{SE} > 200\ \mu m$) was proven to act as the key contributor to viscosity change for FP suspensions. Meanwhile, the fine particle population ($d_{SE} < 200\ \mu m$) was demonstrated as weakly impacting the suspension viscosity. During enzymatic hydrolysis at dilute conditions, the viscosity decreased significantly, mainly due to reductions of particle size, although morphological aspects could also have an effect. At higher solid loading conditions, the role of biomass concentration may become more pronounced. Working on pretreated spruce chips, Wiman et al. [42] also stated the changes in suspension viscosity during enzymatic hydrolysis are due to both factors: fiber properties and water insoluble solid content.

For SCB, the initial population exhibited monomodal distribution of finer size with small spreading compared to FP (Fig. 3A). Considering the curves of Fig. 8, the evolution of $E_v(d_{SE}) \times \Phi_v$ during enzymatic hydrolysis is less pronounced than for FP, but a slight change in particle size was observed despite a reduction of Φ_v. At 3 FPU/g cellulose, a slight increase in size is observed at 1 h and 3 h, although the distribution function was weighted by the volume fraction. This change just follows the viscosity overtaking which was observed at t = 30 min (Fig. 8B). From this point, the evolution of $E_v(d_{SE}) \times \Phi_v$ indicated a reduction in particle volume fraction associated with a shift to lower size. At 0.3 FPU/g cellulose, a slight increase of particle size was observed up to 3 h which then stabilized until t = 12 h (Fig. 8A). This distribution was nearly identical with that of 3 FPU/g cellulose at 1 h. Beyond 3 h, roughly corresponding to the peak in suspension viscosity, the population mainly consisted of coarse particles. The viscosity overtaking was assumed to be related to $E_v(d_{SE}) \times \Phi_v$ evolution. For aggregates corresponding to the biggest particles (Fig. 2B), the release of fibers from aggregates may contribute to a slight shift in PSD, with a moderate increase in particle number (discussed with CLD) and then

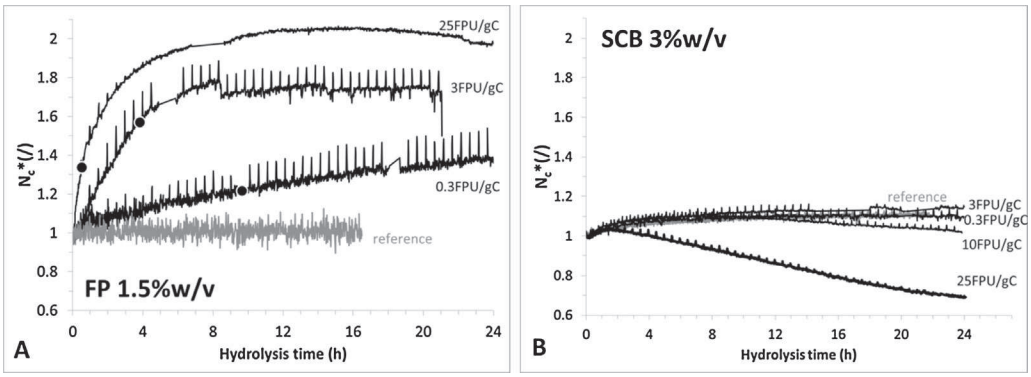

Fig. 9. Evolution in N_c^* during enzymatic hydrolysis of FP 1.5% w/v (A) and SCB 3% w/v (B) for E/S loading ranging from 0.3 up to 25 FPU/g cellulose (•: points beyond which viscosity variations are negligible).

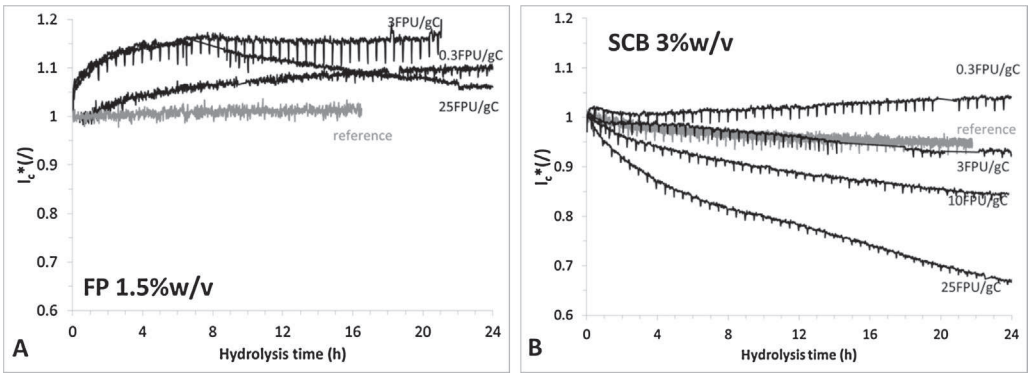

Fig. 10. Evolution in l_c^* during enzymatic hydrolysis of FP 1.5% w/v (A) and SCB 3% w/v (B) for E/S loading ranging from 0.3 up to 25 FPU/g cellulose.

an intensification of particle–particle interaction. It is noticeable that the volume fraction as calculated from the initial concentration and hydrolysis yield (cf. §2.3.2) is different from the effective volume fraction of particles that determines the rheological behavior, especially considering the observed aggregates and fibers with SCB. The volume fractions based on dry matter content and effective object volume are not linked in a simple way, and may exhibit opposite trends. (For instance, the effective object volume can vary when interparticle interactions or particle-solvent interactions are modified by additives).

Many apparent contradictory results can be found in the literature concerning the evolution of viscosity with particle size (for a given concentration or volume fraction). This illustrates the fact that parameters such as particle morphology and/or particle interactions greatly influence rheological behavior [33,35–38]. Moreover, the reason for $E_\nu(d_{SE}) \times \Phi_\nu$ evolution needs to be examined and assumptions may be postulated. It is evident that cellulase enzymes are able to break down cellulosic fibers and solubilize them in order to produce glucose. Basically, this reaction leads to a decrease in particle size. With respect to the granulometry and morphology of pretreated SCB, a considerable number of agglomerates are present. Once enzymes are added to the substrate suspension, both agglomerates and individual particles are attacked at the same time. Biocatalyst actions on agglomerates probably open the structure and extract/separate the fibers from the agglomerates. In this case, an increase in particle size distribution is realistic. In addition, it would lead to a moderate increase in particle number, as well as particle surfaces, in other words, the average distance between particles would be reduced and interactions increased. Consequently, particle-to-particle interactions are enhanced and the suspension viscosity increases. In contrast, the attack of enzymes on individual particles results in a decrease in viscosity due to the solubilization mechanism. In the first stage of hydrolysis, the effect on agglomerates is stronger than the solubilization of small individual particles, causing a growth in suspension viscosity. As concerns the amount of E/S loading, once the de-structuration of agglomerates reaches a threshold where all agglomerates are separated, the suspension viscosity will gradually decrease. An additional phenomenon to explain this overshot in viscosity is linked to particle shape. Giesekus [34] studied the dependence of glass fiber suspension viscosity *versus* length/diameter (L/D) ratios. This research revealed that the relative viscosity rose as the L/D proportion increased, or in other words, a suspension of longer fibers will possess higher viscosity than a suspension of shorter ones. For SCB suspensions, the dispersion of agglomerates into individual fibers can be considered an evolution of particle morphology, from low to high L/D proportion.

3.4.2. In-situ *chord length distribution*

Focusing on the evolution of fine particles, *in-situ* CLD measurements were performed, and normalized quantities were defined as the ratio to their initial values. The evolutions of normalized total chord count, N_c^* and l_c^* are reported in Figs. 9 and 10 respectively, for FP (Fig. A) and SCB (Fig. B).

For FP, both N_c^* (Fig. 9A) and l_c^* (Fig. 10A) indicate growing trends, whereas they remain almost constant in the reference case (no activity, deviation < 5%). Small peaks may be explained by the mixing rate changes, from 100 to 125 min^{-1} every 30 min. Considering N_c analysis, the interpretations will be limited to regions of stable viscosity, *i.e.*, times beyond the markers in Fig. 9A, which correspond to a maximum 25% deviation based on final viscosity. Accounting for DLS volume-weighted distribution (Fig. 3A), the initial FP suspension contained 46% coarse particles and 54% fine

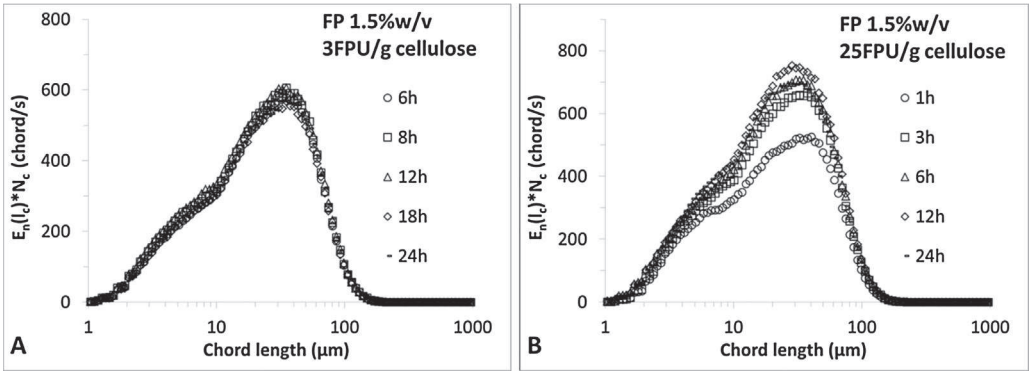

Fig. 11. Evolution of number-weighted chord length distribution multiplied by N_c (FP suspension, 1.5% w/v) during hydrolysis with Ctec2 ratios 3 FPU/g cellulose (A) and 25 FPU/g cellulose (B).

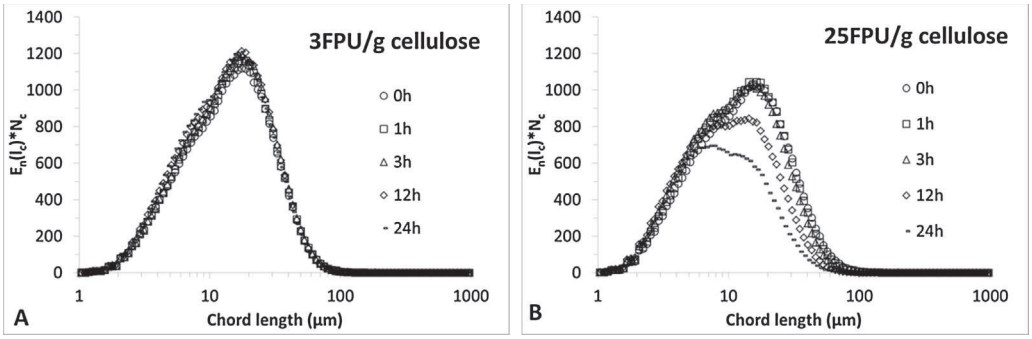

Fig. 12. Evolution of number-weighted chord length distribution multiplied by N_c (SCB suspension, 3% w/v) during hydrolysis with Ctec2 ratios 3 FPU/g cellulose (A) and 25 FPU/g cellulose (B).

ones. A few large fibers possibly account for a considerable volume fraction equivalent to a huge number of fine particles. For number-weighted distribution obtained by FBRM analysis, the fraction of large particles is almost invisible, whereas the finest are well described. During enzymatic attack, different phenomena leading to opposite evolutions of N_c^* and l_c^* are encountered and associated with different mechanisms. The fragmentation of large particles generates a significant growth in number of medium-sized particles while the solubilization of the finest particles leads to a decrease of l_c^*.

For SCB, most of the time N_c^* (Fig. 9B) and l_c^* (Fig. 10B) exhibit opposite trends when compared to FP. Note that viscosity variations are almost negligible, allowing N_c^* interpretation throughout the whole hydrolysis. Biochemical analysis (Fig. 5) confirms the existence of a solubilization mechanism at enzyme loading from 3 FPU/g cellulose. It is suggested that there is a balance between four mechanisms: agglomerate separation, fiber fragmentation, solvation and solubilization. At 0.3 FPU/g cellulose, with only 3.1% glucose yield at 24 h, the effect of solubilization is almost negligible and the fragmentation is not enough to reduce particle size. A swelling effect of substrate by solvation may be responsible for the slight increase in l_c^*. At higher enzyme loading, the separation of agglomerates and the fragmentation of coarse fibers may explain the rise in chord number as well as the fall in mean chord length in the first stage. Then, depending on enzyme dosage, a solubilization mechanism becomes significant and predominant (illustrated by an increase in glucose yield), and both N_c^* and l_c^* exhibit decreasing trends. The coexistence of four mechanisms—separation of agglomerates, fragmentation of coarse fibers, solvation and solubilization of fine ones—is well established and consistent with the enzyme/substrate ratio.

For a better understanding of the enzymatic attack on the finest population, CLD weighted by N_c are reported in Fig. 11A and B for FP (1.5% w/v), and in Fig. 12A and B for SCB (3% w/v) at 3 and 25 FPU/g cellulose.

The interpretation for FP was restricted to the region of stable viscosity ($t \geq 1$ h for 25 FPU/g cellulose, $t \geq 4$ h for 3 FPU/g cellulose and $t \geq 9$ h for 0.3 FPU/g cellulose). As reported in Fig. 11A and B, a significant evolution in particle number was observed for 25 FPU/g cellulose, while almost no change was witnessed for 3 FPU/g cellulose. With number-weighted distribution, the FBRM analysis provides information about the population of fine particles. The trend at low enzyme loading might assume that there was an equilibrium between fragmentation of coarse and solubilization of fine particles, leading to a balance in total fine particles. Thus, by increasing the enzyme loading ratio to 25 FPU/g cellulose, this balance was broken and the evolution was clearly observed, with an increase of 25% in chord number for the fraction of $10 < l_c < 100$ µm between 1 h and 3 h. The increasing trend continued until 12 h, and finally reached 140% compared to t = 1 h. During this time, the fragmentation mechanism seemed to be stronger than solubilization one. Beyond 12 h, the trend was reversed and a fair reduction in number-weighted distribution was observed for the fraction of $10 < l_c < 100$ µm.

For SCB, the fraction of $10 < l_c < 100$ µm was scrutinized in order to be compared to FP. The phenomenon strongly differs, with almost no evolution at 3 FPU/g cellulose. At the highest loading (25 FPU/g cellulose), distribution curves exhibit a sharp evolution. From 0 h to 3 h, no significant variation was quantified. Nevertheless, a decrease of 30.4% and 64.2% were witnessed after 12 h and 24 h respectively. Below 8 µm (the size of the finest particle), a constant shoulder is identified.

With both substrates, evolution in chord population is linked to the balance and relative magnitude of two mechanisms: (i) the fragmentation of coarse particles into smaller insoluble particles that cause a rise in total number of chords, and (ii) the solubilization of

fine particles, which leads to a drop in total chord population. The different phenomena observed between FP and SCB are consistent with their initial morphogranulometric properties. Biochemical results (Fig. 5) confirmed the presence of a solubilization mechanism and sustained the fragmentation mechanism illustrated by PSD and CLD. At 25 FPU/g cellulose, the fragmentation mechanism played a predominant role in FP suspensions that contain considerable amounts of coarse fibers (46% by volume for $d_{SE} > 200\ \mu m$). For SCB suspensions with a lower size spread (96% of the fine particles are inferior to 200 μm), the two mechanisms, fragmentation and solubilization, appear to be balanced at 3 FPU/g cellulose. When enzyme loading is increased up to 25 FPU/g cellulose, this equilibrium is maintained during the first 3 h, and then solubilization becomes the dominant mechanism. This assumption is supported by biochemical results, with glucose yield reaching 53% and 82% for FP and SCB respectively at 25 FPU/g cellulose and 24 h. For FP and SCB, the obtained results suggest that smaller particles are more accessible to enzymatic hydrolysis than larger ones.

4. Conclusions

The relationships between *in-situ* viscosimetry, *in-* and *ex-situ* morphogranulometry (PSD, CLD) and biochemistry were investigated during enzymatic hydrolysis of lignocellulose substrates under semi-dilute conditions (1.5–2 times higher than critical concentrations) using a dedicated, multi-instrumented set-up. These concentrations generate non-Newtonian behaviors and avoid neglecting particle–particle interactions, contrary to dilute conditions. In light of their industrial potentials, two specific substrates (pretreated SCB 3% w/v) and milled FP 1.5% w/v) were scrutinized during hydrolysis by a commercial cocktail (Ctec2, Novozyme) with ratios ranging between 0.3 and 25 FPU/g cellulose. The appropriate and specific mechanisms (*e.g.*, viscosity overtaking) corresponding to different phenomena were revealed and explained *via* biochemical analysis, *ex-situ* PSD, and *in-situ* CLD analysis.

Firstly, the obtained results highlight the strong influence of PSD and dispersion as well as morphology on suspension viscosity. In semi-dilute conditions, suspension viscosity was found to be closely linked to size distribution spreading, and to depend mainly on the fraction of coarse particles. The population of fine particles had almost no effect on viscosity.

Secondly, during enzymatic hydrolysis, four mechanisms were identified: solvation, particle fragmentation, particle solubilization, and agglomerate separation (especially for SCB). Change in suspension viscosity was related to three of them, excluding solubilization, which mainly occurred with the finest population fraction. The increase in suspension viscosity by solvation may be attributed to the swelling effect of lignocellulose fibers, which increases the effective volume fraction. In contrast, the fragmentation mechanism resulted in a collapse of viscosity. The mechanism was explained by the shift in volume fraction of the coarse population, which was known as the determinant factor of viscosity, into fine population. The solubilization mechanism showed almost negligible effect, as the suspension can be totally liquefied at very low bioconversion yield.

Interestingly for suspension that contains agglomerates at low enzyme loading ratios, the separation of agglomerates by both mechanical mixing and enzymatic actions caused a significant viscosity overtaking, which is an unfavorable phenomenon for bioprocess intensification. The mechanism was explained by two assumptions: (i) the separation of agglomerates into individual particles strengthens the interactions between them by increasing the total number of particles in suspension and (ii) the separation induces an evolution of population shape from sphere-like (agglomerate) into fiber-like (individual fragments) that affects the suspension viscosity. At high enzyme loading, the viscosity overtaking was almost non-observable.

From an academic standpoint, the kinetics associated with viscosity, morphology and biochemistry need to be modeled. Bottleneck and balance between these phenomena will be scrutinized by local metrology (*e.g.*, tomography to measure void fraction, specific surface, and enzyme accessibility).

From an industrial standpoint, enzymatic hydrolysis at high dry matter content stands as a major challenge. Thus the activity profile of the cocktail and the physical properties of the substrates are worth considering beyond the merely biochemical yield. In order to minimize transfer limitations (mass, heat, momentum) and ensure adequate mixing and energetic efficiency, for FP and SCB, a high proportion of endoglucanase activity is required to quickly liquefy the substrate *via* a fragmentation mechanism. Monodisperse lignocellulose material has the additional advantage of low suspension viscosity for the bioconversion process.

Conflict of interest

None.

Acknowledgements

This work was supported by TECHNO 1 & 2–Erasmus Mundus (European Commission, project managed by UPS – Toulouse) and HTMS BioAsie (Ministère des Affaires Étrangères et du Développement International, MAEDI, programme BIO-Asie, N° 34082NF). It participated in the ANR Grant ProBio3-Investissement d'Avenir under the contract number ANR-11-BTBR-0003.

Authors are gratefully to the Centre de Traduction – Université Toulouse III-Paul Sabatier for English language review.

References

[1] J.-C. Ogier, D. Ballerini, J.-P. Leygue, L. Rigal3, J. Pourquié, Production d'éthanol à partir de biomasse lignocellulosique, Oil Gas Sci. Technol. 54 (1999) 67–94.
[2] A. Pandey, C.R. Soccol, P. Nigam, V.T. Soccol, Biotechnological potential of agro-industrial residues. I: sugarcane bagasse, Bioresour. Technol. 74 (2000) 69–80.
[3] S. Kim, B.E. Dale, Global potential bioethanol production from wasted crops and crop residues, Biomass Bioenergy 26 (2004) 361–375.
[4] M.L. Carvalho, R. Sousa, U.F. Rodriguez-Zuniga, C.A.G. Suarez, D.S. Rodrigues, R.C. Giordano, R.L.C. Giordano, Kinetic study of the enzymatic hydrolysis of sugarcane bagasse, Braz. J. Chem. Eng. 30 (2013) 437–447.
[5] L.M.F. Gottschalk, R.A. Oliveira, E.P.d.S. Bon, Cellulases, xylanases, β-glucosidase and ferulic acid esterase produced by Trichoderma and Aspergillus act synergistically in the hydrolysis of sugarcane bagasse, Biochem. Eng. J. 51 (2010) 72–78.
[6] X.B. Zhao, L. Dong, L. Chen, D.H. Liu, Batch and multi-step fed-batch enzymatic saccharification of Formiline-pretreated sugarcane bagasse at high solid loadings for high sugar and ethanol titers, Bioresour. Technol. 135 (2013) 350–356.
[7] A.A. Modenbach, S.E. Nokes, Enzymatic hydrolysis of biomass at high-solids loadings—a review, Biomass Bioenerg. 56 (2013) 526–544.
[8] B. Palmqvist, G. Lidén, Torque measurements reveal large process differences between materials during high solid enzymatic hydrolysis of pretreated lignocellulose, Biotechnol. Biofuels 5 (2012) 1–9.
[9] N.V. Pimenova, A.R. Hanley, Effect of corn stover concentration on rheological characteristics, Appl. Biochem. Biotechnol. 113 (2004) 347–360.
[10] J.S. Knutsen, M.W. Liberatore, Rheology of high-solids biomass slurries for biorefinery applications, J. Rheol. 53 (2009) 877–892.
[11] S. Viamajala, J.D. McMillan, D.J. Schell, R.T. Elander, Rheology of corn stover slurries at high solids concentrations—effects of saccharification and particle size, Bioresour. Technol. 100 (2009) 925–934.
[12] B.H. Um, T.R. Hanley, A comparison of simple rheological parameters and simulation data for Zymomonas mobilis fermentation broths with high substrate loading in a 3-L bioreactor, Appl. Biochem. Biotechnol. 145 (2008) 29–38.
[13] R.K. Dasari, R.E. Berson, The effect of particle size on hydrolysis reaction rates and rheological properties in cellulosic slurries, Appl. Biochem. Biotechnol. 137 (2007) 289–299.
[14] S. Rezania, Z.L. Ye, R.E. Berson, Enzymatic saccharification and viscosity of sawdust slurries following ultrasonic particle size reduction, Appl. Biochem. Biotechnol. 153 (2009) 103–115.

[15] J.S. Knutsen, M.W. Liberatore, Rheology modification and enzyme kinetics of high solids cellulosic slurries, Energy Fuels 24 (2010) 3267–3274.
[16] T.-C. Nguyen, D. Anne-Archard, V. Coma, X. Cameleyre, E. Lombard, C. Binet, A. Nouhen, K.A. To, L. Fillaudeau, In situ rheometry of concentrated cellulose fibre suspensions and relationships with enzymatic hydrolysis, Bioresour. Technol. 133 (2013) 563–572.
[17] C.J. Dibble, T.A. Shatova, J.L. Jorgenson, J.J. Stickel, Particle morphology characterization and manipulation in biomass slurries and the effect on rheological properties and enzymatic conversion, Biotechnol. Prog. 27 (2011) 1751–1759.
[18] L.T.C. Pereira, L.T.C. Pereira, R.S.S. Teixeira, E.P.D. Bon, S.P. Freitas, Sugarcane bagasse enzymatic hydrolysis: rheological data as criteria for impeller selection, J. Ind. Microbiol. Biotechnol. 38 (2011) 901–907.
[19] K.W. Dunaway, R.K. Dasari, N.G. Bennett, R. Eric Berson, Characterization of changes in viscosity and insoluble solids content during enzymatic saccharification of pretreated corn stover slurries, Bioresour. Technol. 101 (2010) 3575–3582.
[20] C.C. Geddes, J.J. Peterson, M.T. Mullinnix, S.A. Svoronos, K.T. Shanmugam, L.O. Ingram, Optimizing cellulase usage for improved mixing and rheological properties of acid-pretreated sugarcane bagasse, Bioresour. Technol. 101 (2010) 9128–9136.
[21] H. Jørgensen, J. Vibe-Pedersen, J. Larsen, C. Felby, Liquefaction of lignocellulose at high-solids concentrations, Biotechnol. Bioeng. 96 (2007) 862–870.
[22] C. Cara, M. Moya, I. Ballesteros, M.J. Negro, A. González, E. Ruiz, Influence of solid loading on enzymatic hydrolysis of steam exploded or liquid hot water pretreated olive tree biomass, Process Biochem. 42 (2007) 1003–1009.
[23] C. Roche, C. Dibble, J. Stickel, Laboratory-scale method for enzymatic saccharification of lignocellulosic biomass at high-solids loadings, Biotechnol. Biofuels 2 (2009) 1–11.
[24] J.J. Stickel, J.S. Knutsen, M.W. Liberatore, W. Luu, D.W. Bousfield, D.J. Klingenberg, C.T. Scott, T.W. Root, M.R. Ehrhardt, T.O. Monz, Rheology measurements of a biomass slurry: an inter-laboratory study, Rheol. Acta 48 (2009) 1005–1015.
[25] Y. Liu, J. Xu, Y. Zhang, Z. Yuan, J. Xie, Optimization of high solids fed-batch saccharification of sugarcane bagasse based on system viscosity changes, J. Biotechnol. 211 (2015) 5–9.
[26] J.H. Sánchez, G.C. Quintana, M.E. Fajardo, Rheology of pulp suspensions of bleached sugarcane bagasse: effect of consistency and temperature, Tappi J. 14 (2015) 601–606.
[27] P.J. Van-Soest, Use of detergents in the analysis of fibrous feeds. II. A rapid method for the determination of fiber and lignin, J. A.O.A.C 46 (1963) 829–835.
[28] T.C. Nguyen, In-situ and Ex-situ Multi-scale Physical Metrologies to Investigate the Destructuration Mechanisms of Lignocellulosic Matrices and Release Kinetics of Fermentable Cellulosic Carbon, Ingenieries Microbiennes Et Enzymatiques, Institut National de Sciences Appliquees Toulouse, Toulouse, 2014.
[29] R. Simha, A treatment of the viscosity of concentrated suspensions, J. Appl. Phys. 23 (1952) 1020–1024.
[30] K. Riedel, J. Ritter, K. Bronnenmeier, Synergistic interaction of the Clostridium stercorarium cellulases Avicelase I (CelZ) and Avicelase II (CelY) in the degradation of microcrystalline cellulose, FEMS Microbiol. Lett. 147 (1997) 239–244.
[31] A.B. Metzner, R.E. Otto, Agitation of non-Newtonian fluids, AIChE J. 3 (1957) 3–10.
[32] M. Jahangiri, M.R. Golkar-Narenji, N. Montazerin, S. Savarmand, Investigation of the viscoelastic effect on the metzner and otto coefficient through LDA velocity measurements, Chin. J. Chem. Eng. 9 (2001) 77–83.
[33] T.C. Nguyen, D. Anne-Archard, L. Fillaudeau, Rheology of lignocellulose suspensions and impact of hydrolysis: a review, Adv. Biochem. Eng. Biotechnol. 149 (2015) 325–357.
[34] H. Giesekus, et al., Disperse systems: dependence of rheological properties on the type of flow with implications for food rheology, in: R. Jowitt (Ed.), Physical Properties of Foods, Applied Science Publishers, 1983, Chap. 13.
[35] G.P. Roberts, H.A. Barnes, C. Mackie, Using the microsoft excel solver tool to perform non-linear curve fitting, using a range of non-Newtonian flow curves as examples, Appl. Rheol. 11 (2001) 271–276.
[36] L.J. Correa, A.C. Badino, A.J. Cruz, Power consumption evaluation of different fed-batch strategies for enzymatic hydrolysis of sugarcane bagasse, Bioprocess Biosyst. Eng. 39 (2016) 825–833.
[37] J.R. Samaniuk, C.T. Scott, T.W. Root, D.J. Klingenberg, Effects of process variables on the yield stress of rheologically modified biomass, Rheol. Acta 54 (2015) 941–949.
[38] G. Radeva, I. Valchev, S. Petrin, E. Valcheva, P. Tsekova, Kinetic model of enzymatic hydrolysis of steam-exploded wheat straw, Carbohydr. Polym. 87 (2012) 1280–1285.
[39] B.B. Derakhshandeh, R.J. Kerekes, S.G. Hatzikiriakos, C.P.J. Bennington, Rheology of pulp fibre suspensions: a critical review, Chem. Eng. Sci. 66 (2011) 3460–3470.
[40] L. Rosgaard, P. Andric, K. Dam-Johansen, S. Pedersen, A.S. Meyer, Effects of substrate loading on enzymatic hydrolysis and viscosity of pretreated barley straw, Appl. Biochem. Biotechnol. 143 (2007) 27–40.
[41] N. Szijártó, M. Siika-aho, T. Sontag-Strohm, L. Viikari, Liquefaction of hydrothermally pretreated wheat straw at high-solids content by purified Trichoderma enzymes, Bioresour. Technol. 102 (2011) 1968–1974.
[42] M. Wiman, B. Palqvist, E. Tornberg, G. Liden, Rheological characterization of dilute acid pretreted softwood, Biotechnol. Bioeng. 100 (2011) 1031–1041.